

Recycling of eps foam and demolition wastes in the preparation of ecofriendly render mortars with thermal-acoustic insulation properties

✉C.D. Acevedo-Sánchez^a, ✉M.A. Villaquirán-Caicedo^b✉, ✉L.F. Marmolejo-Rebellón^a

a. Environmental Pollution Study and Control Group, School of Natural Resources and Environment Engineering, Universidad del Valle, (Cali, Colombia)

b. Composite Materials Group, School of Materials Engineering, Universidad del Valle, (Cali, Colombia)

✉: monica.villaquiran@correounivalle.edu.co

Received 22 December 2022

Accepted 13 April 2023

Available on line 8 August 2023

ABSTRACT: The design of render-mortars from construction and demolition waste (CDW) was evaluated. Fine aggregates from red-clay-brick waste, mortar and concrete waste were used, together with recycled expanded-polystyrene (EPS) as lightweight filler. Mixes composed of 70%-recycled aggregates, and 30% consisting of a matrix of Portland cement were produced. Characterization tests were conducted on the physical, mechanical, thermal, and acoustic properties. The render-mortar A4, A7 and A9 can be classified according to compressive strength results as CSI-W0 for interior use under standard UNE-EN-998-1. The A7 mortar, with the best physical and mechanical results, contained 21% EPS, 17.5% brick waste and 17.5% mortar waste. Mix A4 obtained the lowest thermal conductivity, 0.12 W/m·K - a reduction of 79% compared to the commercial-mortar AC1. The acoustic absorption properties were also enhanced by the incorporation of EPS, such that the A4, A7, and A9 mixes were identified as *Absorbent* for the frequencies of 2000 Hz and 4000 Hz.

KEY WORDS: Interior render mortar; Composite; Demolition waste; Recycling; Circular economy.

Citation/Citar como: Acevedo-Sánchez, C.D.; Villaquirán-Caicedo, M.A.; Marmolejo-Rebellón, L.F. (2023) Recycling of eps foam and demolition wastes in the preparation of ecofriendly render mortars with thermal-acoustic insulation properties. *Mater. Construcc.* 73 [351], e317. <https://doi.org/10.3989/mc.2023.342422>.

RESUMEN: *Reciclado de espuma de EPS y residuos de construcción y demolición en la preparación de morteros de revestimiento eco-amigables con propiedades termo-acústicas.* Se evaluó el diseño de morteros de revestimiento a partir de residuos de demolición. Áridos finos obtenidos a partir de residuos de ladrillos de arcilla cocida, morteros y hormigones se usaron en conjunto con árido ligero de espuma de poliestireno expandido (EPS). Se obtuvieron mezclas compuestas de 70% de agregado reciclado y 30% de matriz de cemento portland, y se desarrollaron pruebas de caracterización físicas, mecánicas, térmicas y acústicas. Los morteros A4, A7 y A9 pueden clasificarse como tipo CSI-W0 para uso interior acorde con la norma UNE-EN-998-1. El mortero A7, con mejores resultados físicos y mecánicos contiene 21% EPS, 17.5% residuos de ladrillo, y 17.5% residuos de mortero. La mezcla A4 obtuvo la más baja conductividad térmica, 0.12 W/m·K – una reducción del 79% comparada con el mortero comercial AC1. La capacidad de absorción acústica también se mejoró por la incorporación de EPS y las mezclas A4, A7 y A9 fueron identificadas como absorbentes para frecuencias entre 2000 – 4000 Hz.

PALABRAS CLAVE: Mortero de interior; Compuesto; Residuos de demolición; Reciclaje; Económica circular.

Copyright: ©2023 CSIC. This is an open-access article distributed under the terms of the Creative Commons Attribution 4.0 International (CC BY 4.0) License.

1. INTRODUCTION

The building industry is among the biggest consumers of natural resources. This sector is considered to cause a great environmental impact, and for generates enormous quantities of waste that reaches landfills. The different wastes are generated during the construction of civil works such as roads, bridges and housing and during the demolition of infrastructure and buildings, when they have reached the end of their useful life, or for reasons of remodeling (1-3). Approximately 10 billion tons of CDW, it is estimated, are generated worldwide each year. Of this, the United States contributes approximately 700 million tons, China around 2.3 *billion* tons, and the European Union more than 800 million tons (4). Every year, it is estimated 615 million tons of CDW is generated around the world, illegal dumping is the most economical alternative makes the dumping of constructions and demolitions debris along streets, and river is not an uncommon sight (5). The CDW occupies 12% of the world's municipal solid waste, moreover, most of CDW waste ends up in landfill, generating the saturation of landfilled sites, which is responsible for the environment pollution (6). The CDW are materials of great interest because of their large volume generated worldwide and because the levels of use do not reach 30% globally and the waste minimization strategies are generally based on the reduction, reuse and recycle to reduce the volume of CDW generated every year around the world (7). The capacity to reuse and recycle CDW depends on the feasibility to sort the different components and to ensure their competitiveness with new materials, in respect to residual contamination and production costs. Important efforts have been deployed over the last decades to identify, develop and implement efficient recycling processes as screening, magnetic separation, manual sorting, optical sorting, crushing and separation of lightweight material by air classification, and design of and mobile plant design to facilitate mobility and lower processing costs (7-10). In general, for Latin American countries - Colombia included - the problem with CDW generation can be attributed to inefficient use and the lack of suitable policies for handling and managing CDW. The different sectors of society must therefore direct efforts towards searching for comprehensive solutions, amongst which Circular Economy strategies can be put forward in the construction sector that encompass the entire life cycle of materials, making use of the concepts of Industrial Ecology such as Industrial Symbiosis and By-product Synergy, so that the waste from the construction industry becomes the raw material of this sector or of other industrial sectors (3). Although it is estimated recycled aggregate could save natural sources and reduce environmental pollution, its inferior quality compared to virgin ones, such as low density, high porosity, high water absorption rate, and micro-cracks

in ITZ (11). Nevertheless, mortars produced with recycled aggregate from CDW have obtained adequate physical and mechanical properties, due to the adequate distribution of the grain size and to the greater content of fines present (12). As such, in recent years, research has been carried out on incorporating recycled aggregates from CDW for mortars and concrete. Recycled coarse aggregate dosage in conventional or high-performance concrete, producing good quality construction materials at a reasonable cost and with a lower environmental impact (13, 14).

Different researchers have found the recycled aggregates have a highwater absorption rate (15) which causes the free water in the mortar mix to be absorbed by the recycled aggregates. The data shows that as the percent recycled aggregates fines increases in mortar, the consistency decreases linearly (15). Specifically, rendering mortars elaborated with CDW have shown presence of cracking due to capillary stresses, these can be controlled by reduce the fines content, the grain size distribution, and the effective water/cement ratio (16). Particle size distribution and shape of CDW greatly influence the ratio of voids within the mortar, thus conditioning its performance (12). As the void ratio decreases so less binder and water is required to make a mortar, and then shrinkage also decreases (17). On the case of concrete elaborate with red clay brick wastes, a higher water absorption and porosity, reflected in changes in the consistency of the concrete (18). Incorporation of fine recycled aggregates and CDW powder has been evaluated, finding improvements in mechanical properties with the incorporation of fine concrete aggregates (< 0.149 mm) (19) and mixed recycled aggregate powders (20). Nevertheless, the physical, mechanical, and durability properties of newly produced concrete are significantly affected by many properties of recycled, such as amount, compressive strength, abrasion resistance, water absorption, density, size, particle size distribution, and shape (11).

The non-stone-derived wastes that are most difficult to manage, on completing their useful life, expanded polystyrene (EPS) features prominently, unlike other plastics, it is challenging to get back in its base form. The recycling process required to reform foam blocks, and the entire process is time-consuming and expensive, thus, the majority of commercial and curbside waste management companies require its disposal in the trash can, and finally in landfills due to its low density and high air content (95%) (21). According to Environmental Protection Agency (EPA), in 2018 in USA 14.5 million tons of plastic container and packaging were generated, and over 69% was landfilled (22). The problem associated with its generation is that it fulfills its industrial function very quickly and soon ends up as part of the accumulation of solid waste (21, 23). It is also chemically inert and a non-biodegradable material (24). On the other hand, improving the energy efficiency of machinery

and premises is one of the most important ways of achieving global energy sustainability. Energy that is not used is the cheapest energy of all, and buildings are large consumer of thermal energy. In fact, the residential and services sectors account for 27% of the total energy consumed in the Europe Union, and much of this energy is used in air conditioning (25). Lightweight materials have been used to improve the thermal efficiency, the incorporating of low-density clay bricks (25), vermiculite particles (26, 27) and EPS-based composites showed improvement in acoustic and thermal insulation (21, 28-30). However, there is not reports about utilization of EPS residues together CDW for preparation of render mortar.

This research reported the results of producing an interior render mortar made from mixtures of other of wastes – red clay brick, concrete demolition as fine aggregates and sanded EPS – and evaluated the influence of incorporating waste materials on the mechanical, thermal, physical, and acoustic properties, to obtain a sustainability composite material that offers greater living comfort to interior homes, while contributing to the circular economy.

2. EXPERIMENTAL METHODOLOGY

2.1. Starting materials

General use Portland cement was used, the CDW used in this research were selected and sampled from the waste storage yard of MAECOL®, Materiales Ecológicos de Colombia SAS, located in Yumbo, Colombia. The materials came from various work in building in the city of Cali. Specifically, fired red clay brick waste (BW) and mortar and concrete waste (MW) were used, which underwent crushing in a jaw mill followed by milling in a hammer mill. The resulting material (Figure 1) was sifted through a No. 30 mesh sieve, and the retained material was used for this research.

Expanded polystyrene (EPS) waste was selected and samples taken from a building site in the city of Cali (Constructora Bolívar, Colombia). The EPS was collected in the form of blocks and was used in forming slab caissons. The EPS was sanded in an in-

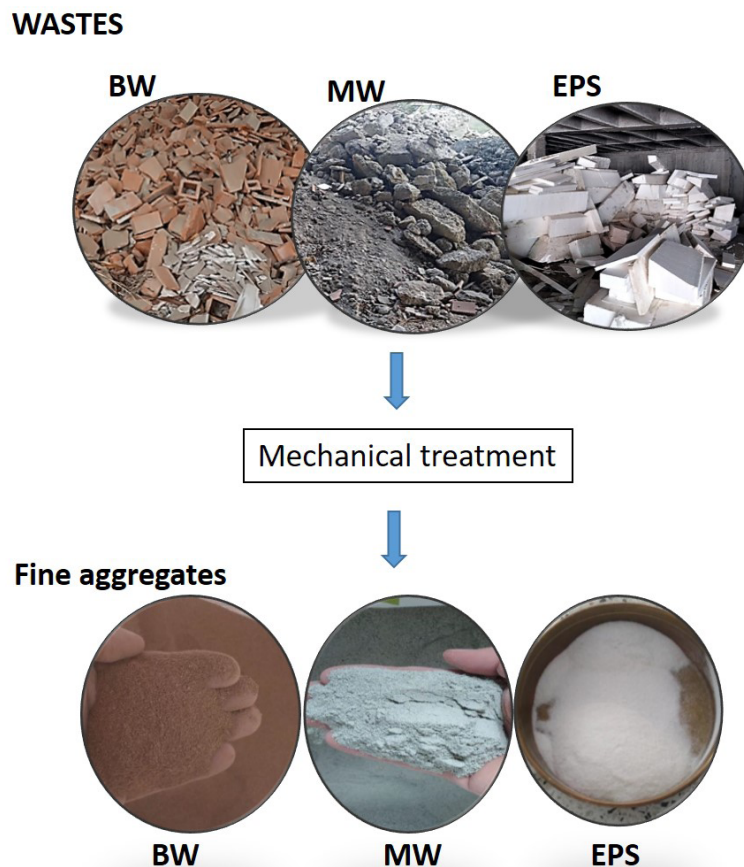


FIGURE 1. Raw materials and fine aggregates for render mixtures.

dustrial sander (Trofemarcas, Colombia) at a speed of 330 m/min and with a No. 60 sandpaper. The sanded EPS was sieved in a No. 50 mesh sieve, and the retained material used for this study.

2.2. Tests and characterization techniques

The following characterization techniques were used:

- The particle size distribution of the raw materials was determined by laser particle size analyzer (Mastersizer 2000, Malvern Panalytical). The density and absorption of fine aggregates BW and MW was testing according to ASTM C128. In the case of sanded EPS residue, the “Unit Weight” was determined with a graduated cylinder, which was filled to a volume of 54 ml, then the sanded EPS was weighed. Observation of the particle morphology and optimized mixing with CDW-EPS was carried out in a JEOL scanning electron microscope (SEM), Ref: JSM-6490LV, high vacuum (3×10^{-6} torr) and accelerating voltage at 20 kV. The equipment has an INCAPentaFETx3 Model 7573 detector (Oxford Instruments). Additionally, the EDS analysis unit was used to determine the semi-quantitative chemical composition of the materials evaluated. The powder raw materials and pieces resulting from the compressive strength test were metalized in a Denton Vacuum Desk IV tank on a gold plate which was deposited for later observation.
- Compressive strength was evaluated at 7 and 28 days, using a Tinius Olsen testing machine with a capacity of 50 kN at a test speed of 1 mm/min, under the ASTM C109/C109M-10 standard. For each mix, three specimens were tested, according to the standard method.
- Adherence was evaluated at 28 days, using the same universal testing machine, by adapting the ASTM C932 standard method. For each mix, six specimens were tested; in this test, the mortars designed with waste materials were adhered to a mortar consisting of cement:sand in a 1:3 ratio, liquid/solid ratio of 0.26, whose compressive strength is 17.7 MPa.
- Apparent density, water absorption, and permeable pore volume percentage were evaluated according to the ASTM C642 standard method.
- Setting time was evaluated using the Vicat Apparatus. This test was performed following Colombian technical standard NTC118. The drying time of optimized mortars was determined comparatively on applying it to an interior brick wall of the laboratory. Initial dry time is when the material is applied in a first coat until the second coat can be used. The feel of the applicator determines this time. The final drying time is the time interval from when the last layer of material is applied until the cloth is completely dry to the touch.

- The test to determine the conductivity, thermal diffusivity and specific heat of the mixes was carried out in the Hot Disk Thermal Constant Analyzer, model TPS 500 S, following the ISO 22007-2 standard. For this test, cubic geometry samples of 50 mm x 50 mm x 15 mm were used.
- The measurement of acoustic properties test was carried out following the recommendations of other authors (31-33) as an alternative method to the impedance tube. An Alexis model M1520 active monitor was used as a frequency emission source. A Beyedynamic microphone, model MM1, with condenser and omnidirectional polar pattern was used, with a measurement range between 50 Hz and 16,000 Hz. The Solid State Logic interface model SSL2+ and the Smaart V8 software were employed.

Additionally, application of the optimal mixes was carried out on the surface of a wall to determine the characteristics of material consumption, workability during application, drying time and finally visual monitoring was carried out up to 60 days after application.

3. RESULTS AND ANALYSIS

3.1. Raw materials

Figure 2 shows the particle size distribution curves for the waste used, BW, MW and EPS. The average particle size for BW and MW was 322.2 μm and 222.3 μm , respectively, and in the case of EPS it was 385.4 μm . The density of Portland cement is provided by the manufacturer technical data sheet, which is 2411 Kg/m^3 . The apparent density was 2550 Kg/m^3 and 1870 Kg/m^3 for BW and MW respectively; and the absorption was 2.11% for BW, and 12.35% for MW. The “Unit Weight” for EPS sanded was 140 Kg/m^3 .

The Figure 3 presents the SEM images for the waste materials under study. The MW powders (Figure 3a and b) are composed of particles of irregular shapes and different sizes, some less than 100 μm , which corroborates what was found in the laser granulometry for this waste. Also observed in Figure 4a is the presence of cement paste with many micropores adhered to large-sized particles. Other studies have shown that a higher content of adhered mortar influences a greater water absorption and a decrease in the density (34-36). In Figure 3c and d, the BW powders are shown. These are made up of angular and irregular particles of different sizes, corroborating the broad size distribution previously shown in the Figure 3a. For higher increases in the BW particle (Figure 5d), it is possible to observe an irregular and vitreous surface of the particles due to brick firing temperatures around 800-900 $^{\circ}\text{C}$.

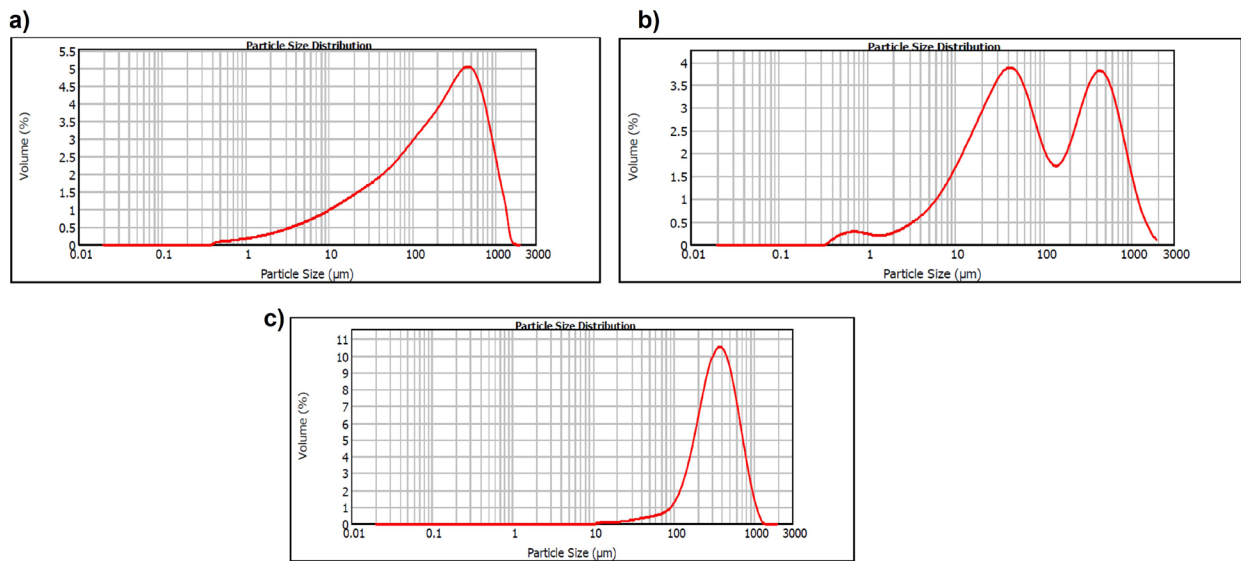


FIGURE 2. Particle size distribution curves for the waste materials used as fine aggregates (a) BW, (b) MW and (c) EPS.

The lightweight EPS filler, after the sanding process, presented a wrinkled and/or rolled plate-like morphology (Figure 3e and f), which can be attributed to the sanding process at high revolutions. The higher magnification image (Figure 3f) shows that the wall of the initial foam has been modified and after sanding, crushing of the cells was generated. The EDS results indicated in Figure 3b and 3d are shown in Table 1, corroborating the aluminum-silicate nature for BW and MW.

3.2. Mix design

The render mortars were made from 70% by volume recycled fine aggregates (BW, MW and EPS) and 30% by volume matrix (99.7 wt% general use Portland cement and 0.30 wt% methyl hydroxyethyl cellulose powder (Cellueast™ FM ME 40000) for improving the workability of plaster when applied on a wall. The matrix content remained fixed, and within the 70% that constitutes aggregates, different combi-

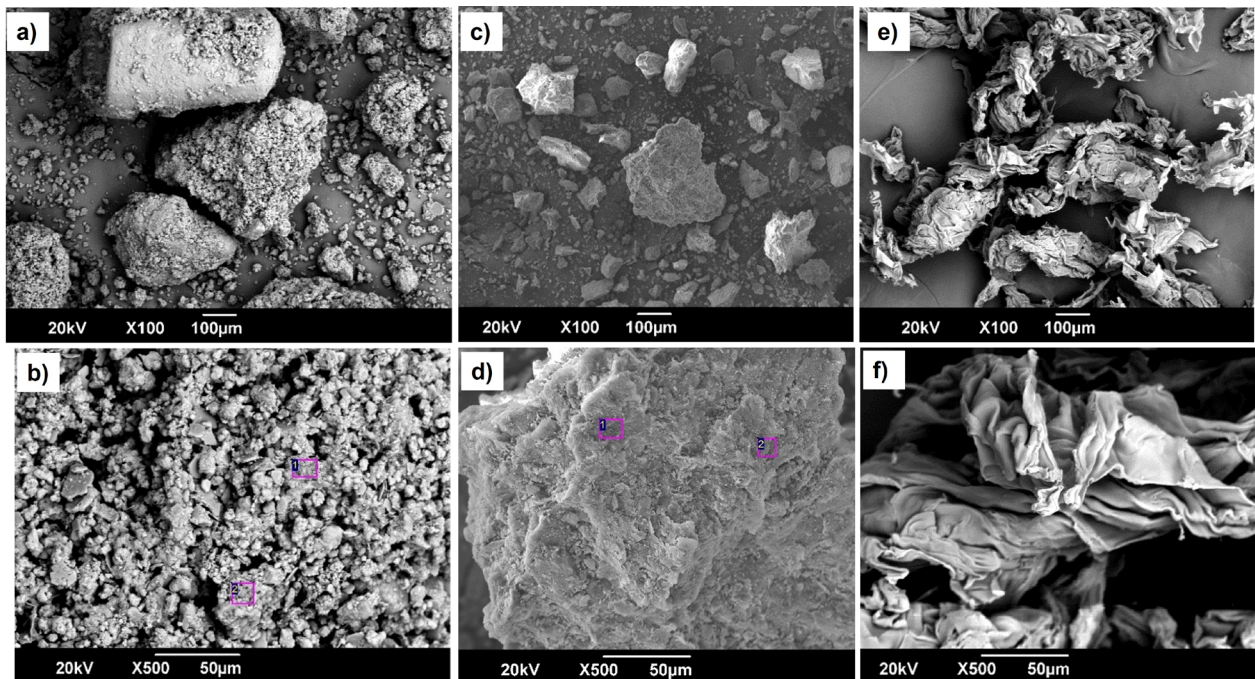


FIGURE 3. SEM images (mode: BSE) of the waste materials under study: (a) and (b) MW, (c) and (d) BW, (e) and (f) sanded EPS.

TABLE 1. Chemical composition of BW and MW waste samples.

BW	Element	Point 1 (wt %)	Point 2 (wt %)
	O	29.46	20.81
	Al	17.76	19.07
	Si	37.52	28.16
	Fe	15.25	31.96
MW	Element	Point 1 (wt %)	Point 2 (wt %)
	O	36.53	42.36
	Si	11.38	15.45
	Ca	36.19	42.19
	Br	7.75	

nations were used following the EPS/CDW volume proportionality of 70/30 (mix A1), 50/50 (mixes A4, A5 and A6) and 30/70 (mixes A7, A8 and A9) for a total of 7 mixes (Figure 4 and Table 2). Additionally, as a commercial render mortar from IMPADOC® was used, labelled AC1.

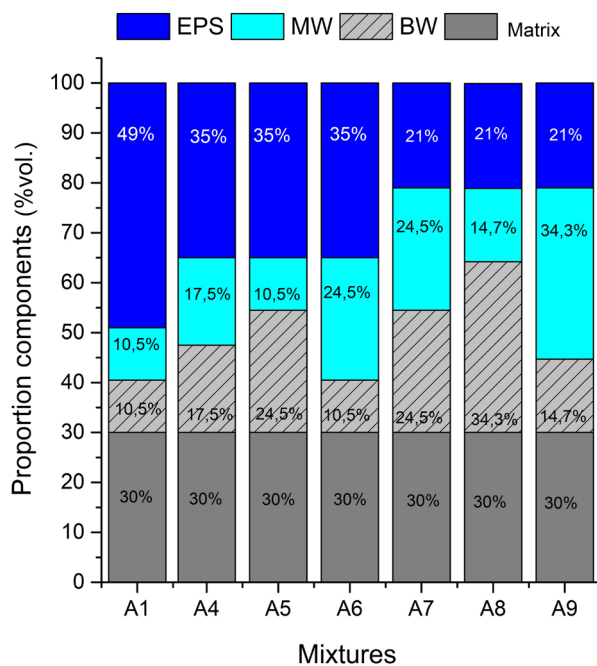


FIGURE 4. Proportions (in volume) of the elaborated mixes.

Water content was adjusted to achieve a constant workability among all mixes, which was similar to that required during the application of the commercial render mortar AC1. The total water to cement ratio (w/c) for the mortars was defined as that required for obtaining a consistency (measured on flow table) similar to AC1 (94 mm). Table 3 shows the water content needed for each mix. The high-water requirement is related to the morphology (pronounced angularity), higher absorption and more porous surface for recycled aggregates particles after the crushing process (18) which will be observed later in the microscopy images. Previously, has been reported that mortar with EPS required a higher content of mixing (28). In general, the high-water requirement in the mixes caused a slow setting process, which led to the decision to leave the mixes hardening at ambient laboratory conditions (relative humidity 70%, temperature 25 °C).

3.3. Mechanical and physical performance of the render mortars produced

In Figure 5a, the compressive strength results for the proposed mixes are shown. The UNE EN 998-1-2018 standard classifies the render mortar according to compressive strength at 28 days (CS), and water capillary (W). The mortar for interior render application, do not required permeable specification (W0), and compressive strength must be: CS I (0.4-2.5 MPa), CS II (1.5-5.0 MPa), CS III (3.5-7.5 MPa), CS

TABLE 2. Proportions in weight for mixtures.

Component	A1	A4	A5	A6	A7	A8	A9
Cement, (Kg)	299.1	299.1	299.1	299.1	299.1	299.1	299.1
Cellueast™, (Kg)	0.9	0.9	0.9	0.9	0.9	0.9	0.9
EPS, (Kg)	68.6	49	49	49	29.4	29.4	29.4
BW, (Kg)	267.75	446.25	267.75	624.75	624.75	274.85	874.75
MW, (Kg)	196.35	327.25	458.15	196.35	458.15	641.41	274.89

TABLE 3. Water requirement for the proposed render mortar mixes.

Mix ID	A1	A4	A5	A6	A7	A8	A9	AC1
(%vol. EPS)	49	35	35	35	21	21	21	0
solid: water (parts by weight)	1: 1.58	1: 0.97	1: 0.88	1: 1.01	1: 0.63	1: 0.56	1: 0.60	1: 0.45

IV (≥ 6 MPa). Mixes A1, A5 and A6 did not reach the minimum value of 0.4 MPa contemplated in the standard to be classified as an interior render mortar. In those mixtures, the results show that increasing the EPS content directly affects the mechanical properties of the mix, due to the strength close to zero of the EPS particles and their high compressibility. Different authors have shown that, on using EPS, microcracks are generated in the interfacial transition zone (ITZ) between the aggregate particles and the cement paste, further weakening the mixes (1, 37). It is important to clarify that other researchers have produced render mortars with compressive strengths between 2.5-14.5 MPa using different percentages of recycled aggregates (16, 18, 28) employing EPS-recycled filler can achieve compressive strength between 2.3-2.9 MPa for hydraulic lime mortars.

The A4 mortar (with the same total proportion of BW and MW) gave the highest compressive strength (0.48 MPa) from 35% EPS group. Similarly, for the group of mixes with 21% EPS (A7, A8, A9), the A7 mortar was found to have the highest compressive strength (1 MPa); like A4, it has the same proportion of BW and MW waste in its composition. These results can be explained: (i) via a better balance in the particle size distributions, exhibited increased packing, where the MW waste contributes a greater amount of fine particles with $d(0.5) = 69.1 \mu\text{m}$, while the brick waste BW provides coarser particles with $d(0.5) = 197 \mu\text{m}$, similar results have been shown previously (18). Also, (ii) the equal distribution in volume between the BW and MW wastes in the A4 and A7 mixes; the finest fraction of the BW could also be contributing pozzolanic activity, by reacting with the portlandite from OPC hydration process of the matrix, a behavior that has been previously reported (18, 38). Nevertheless, the compressive strength results for the mixes proposed in this study were lower than for the commercial sample, AC1 (3.05 MPa). In general, the strength of the mortars decreases up to 50% with the replacement of the aggregate due to the high absorption capacity in mixtures with recycled aggregates (20, 39, 40). Additionally, the values of compressive strength in this study are similar to values for EPS-gypsum composites (30, 41), and vermiculite-gypsum composites (26), and higher than vermiculite-gypsum-sunflower stalk fiber composites (27).

The results of adherence test for mixtures is shown in Figure 5b. Mixes A4, A5 and A6 with EPS content

of 35% had a lower adherence compared to A7, A8, A9 (21% EPS), which indicates that there is an inverse proportional relationship between the EPS content in the mix and the adhesive strength the material can acquire once applied. It can also be seen that the adhesive values change markedly in the group of mixes A7, A8, and A9, depending on the variation in the content of BW and MW wastes, adhesive strength found to be greater in A7 (equal volumes of BW and MW waste), followed by mix A9 (a higher volume of MW) compared to mix A8. Just as was explained previously, by eliminating the fine material adhered to the coarse particle, this could contribute to the improved performance in adhesive strength. Adhesive strength values of 0.25 to 0.7 MPa have been found in render mortar by utilization of recycled sand (16-18, 40, 42). (17) and (20) have found that the use of CDW with an average size smaller than $150 \mu\text{m}$ increases the shrinkage in mortars by 44% compared to that in mortars made with natural aggregates, and this increases their cracking, affecting the mechanical strength. These results follow other previous studies where the adherence strength between 0.13-0.23 MPa employing EPS-recycled filler (28). From the above, it is concluded that the higher the EPS content in the mix, the lower the mechanical properties, in agreement with various authors (1, 37). From ANOVA (Table 4) analysis for adherence test show differences between the mixtures. The ANOVA concludes that there is significant evidence that every mixtures influences the levels of adherence. This is how the contrasts showed differences in the combinations of A4-A7, A4-A8, A4-A9, A7-A8, and A7-A9 mixtures—opposite case between mixes A8 and A9. Mixes A7, A8 and A9 presented the most outstanding results, reaching values between 0.044 and 0.085 MPa. The Figure 6. shows specimens A6, A7 and AC1 after the adhesive test. The A6 mixture had an adhesive mode failure, indicating little adhesion between the render mixture and the substrate. While the A7 mixture had a cohesive mode failure, indicating that the render mixture had satisfactory adhesion to the substrate. AC1 has a mixed type failed.

3.4. Density, water absorption, and porosity properties

The low density, higher angularity, and surface roughness of recycled aggregate particles compared

TABLE 4. Analysis of Variance (ANOVA) for response surface quadratic model for adhesive strength R^2 0.9225.

Source	P Adj.	Std. Error	Pr (> t)	
A4-A7	0.00005	0.0051	3.71E-06	Significance
A4-A8	0.02850	0.0051	0.000329	
A4-A9	0.00599	0.0089	0.177398	
A7-A8	0.00139	0.0051	0.401374	
A7-A9	0.00550			
A8-A9	0.65216			No significance
Degrees of freedom	8	Pure Error	0.009	
t value	31.76	Residual error	0.008851	

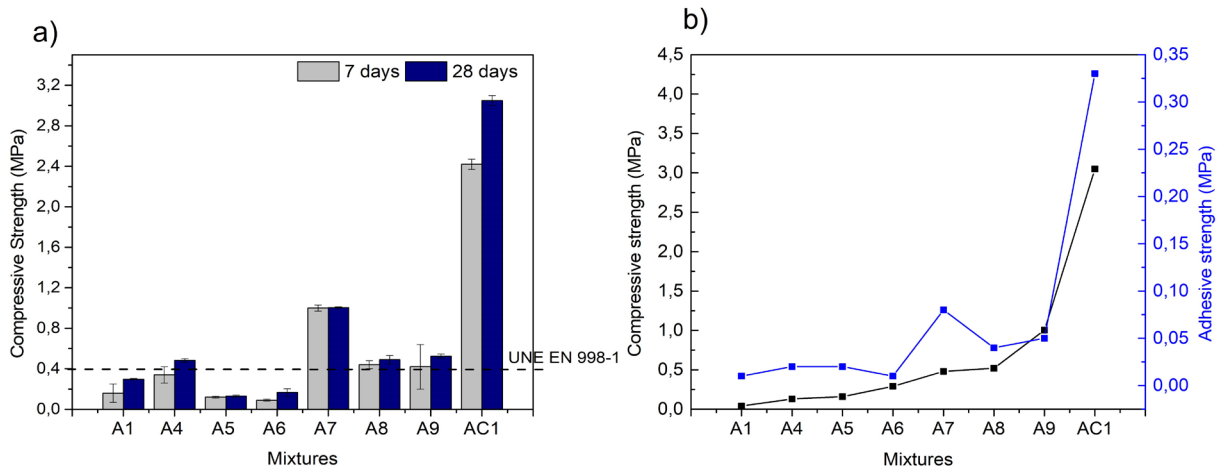


FIGURE 5. (a) Compressive strength of the mixes at 7 and 28 days of curing and (b) adhesive strength.

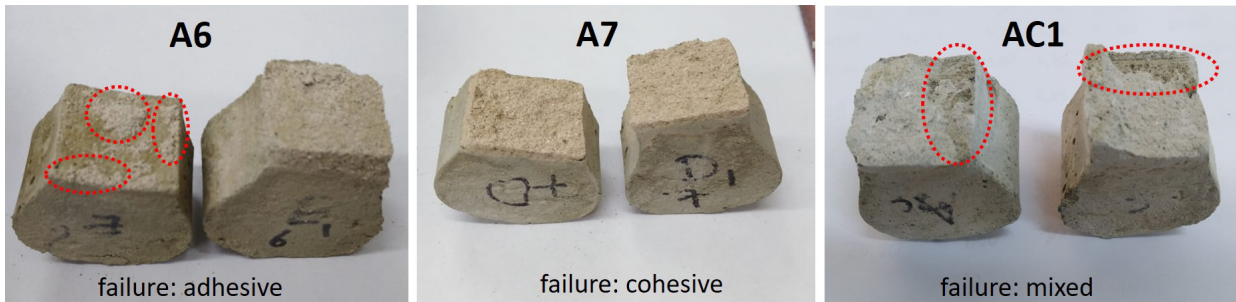


FIGURE 6. Type of failure in mixtures A6, A7 and AC1.

to natural crushed ones play an important role in reducing the density and poorer workability of concrete mixtures (11, 15, 35). The results of density, water absorption and porosity are shown in Table 5. The high-water absorption of the mortars under study stands out, reaching values between 56.2% and 103.5%. A directly proportional relationship was found between the increase in EPS content and water absorption. High water absorption and high porosity in recycled aggregates results in a significant decrease in compressive strength in mortars, as previously has been observed (20, 43). The group of mixes A4, A5, A6 thus had a greater absorption compared to mixes

A7, A8, A9. The porosity in the mixes was higher to the extent that the EPS, MW and BW waste (highly porous waste) was incorporated, which is associated with different phenomena such as: (i) the greater demand for water in the mixes (Table 3) to achieve adequate workability (as explained in the Methodology section) as the EPS was increased. Moreover, as is known, the water that does not react with the OPC matrix is finally released during drying, leaving behind porosity, which in turn is reflected in the greater water absorption for the mixes with 35% EPS compared to the samples with 21%EPS. In addition, it is possible that during the test, the water was trapped

inside the channels of the EPS waste, which were observed to be deep and flattened (SEM, Figure 3e and 3f), and inside the pores of the recycled MW and BW aggregates (Figure 3 a,b,c,d), phenomena that have been reported by other authors (19, 20). Finally, the higher the EPS content, the lower the density of the mixes, and in all cases the density was lower than that of commercial AC1.

The densities of mixes A4, A5, A6 are close to the density of water (1000 Kg/m³), and during the test they initially floated in water, similar to that reported by materials based on gypsum. For a render mortar, a low density can become a technical advantage, since it gives less weight to the packed material, which favors transport, workability, as well as a possible lower consumption of material compared to traditional mortars, which is discussed later in Section 3.8. (15, 40) have found a linear fall of the density of hardened mortar as the replacement ratio of recycled sand increased, which was due to the lower density of recycled aggregate. The density values are lower than EPS-lime mortars (28) and similar to EPS-plaster mortar (44).

According to the previous results of mechanical and physical properties, mixes A4, A7, and A9 were selected for the next part of the study to determine their thermal and acoustic properties.

3.5. Microstructure

The A7 mortar presented the best results in terms of mechanical properties, which indicates a better internal cohesion between the aggregates that compose it and the cement matrix. In Figure 7a an EPS particle can be seen adhered to the mortar, and in Figure 7b the interface between the EPS particle and the cement paste can be seen, indicating that it is of good quality, dense, without presence of microcracks, and in this study the anchoring mechanical type is favored owing to the morphology of the EPS particle. This is in contrast with other studies in which, when EPS with rounded morphology and sizes from 2.0 mm were used, a weak interface and the appearance of microcracks were reported (1, 29, 37). In this investigation, a quality and dense interface was found, associated with the fineness, and elongated morphology that the EPS particles retained after mechanical polishing. The mechanical anchoring of the EPS particle to the matrix, added to the use of a polymer-based additive, to improve adherence and dispersion in the formulation, allows a better anchoring of the EPS.

Table 6 shows the chemical composition results by EDS for mix A7 according to the position where EDS analyses were carried out in Figure 7b. The EDS for point 1 and 2, correspond to the elements that con-

TABLE 5. Results of density, absorption, and porosity for mortar mixtures.

Mix (%EPS)	A1	A4 (35%)	A5 (35%)	A6 (35%)	A7 (21%)	A8 (21%)	A9 (21%)	AC1
Permeable pores (%)	64.75	53.93	53.75	57.97	52.01	52.71	48.90	45.45
Water absorption (%)	115.64	90.70	92.70	103.48	63.66	56.20	59.67	32.25
Apparent density (Kg/m ³)	1240	1380	1350	1430	1770	1920	1590	2420

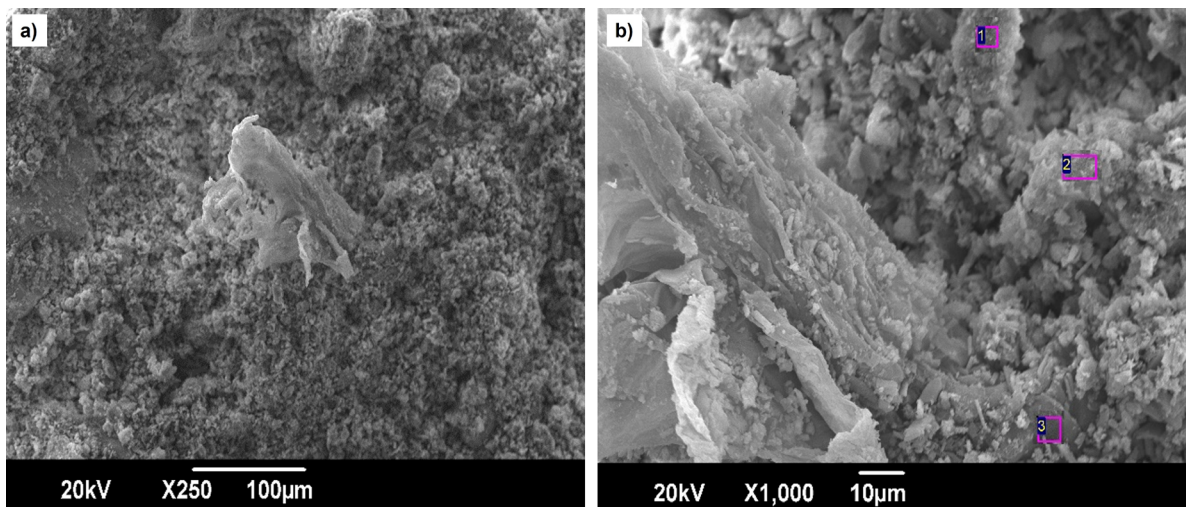


FIGURE 7. SEM (mode: secondary electron) and EDS marked point for the A7 mix at 28 days.

stitute the compounds formed in the hydration of the cement and its reaction with the compounds of silica, aluminum and iron present in the waste of mainly ceramic origin (SiO_2 , Al_2O_3 , and Fe_2O_3), which upon contact with calcium hydroxides (Portlandite, $\text{Ca}(\text{OH})_2$), a product of cement hydration, form compounds such as calcium silicate hydrates (CSH) and calcium aluminates (C_3A). In point 3, meanwhile, located between the junction of the EPS particle and the matrix, the constituent elements are C, O and Ca, which indicates the presence of portlandite, and also the carbon from the EPS.

TABLE 6. EDS of the A7 mix sample.

Element	Point 1 (% by weight)	Point 2 (% by weight)	Point 3 (% by weight)
C	9.15	12.46	43.80
O	41.97	53.51	42.10
Al	8.00	1.71	
Si	11.29	9.81	
Ca	22.35	20.73	14.11
Fe	7.25	1.79	
Identification	Gel CSH	Gel CSH	EPS

Assessment of the physical and mechanical properties made it possible to define mixes A4, A7 and A9 as optimal. The A7 mix was selected for having the best mechanical properties. In the adherence test, however, no significant differences were found between mixes A8 and A9, which both have 21% EPS content. Mix A9 was therefore selected from these two mixes, which had slightly better performance in mechanical properties. Mix A4 was considered for the next stage due to its high content of EPS (35%), which is expected to favor thermal and acoustic performance.

3.6. Thermal properties

Since the EPS has low conductivity (0.030 W/m·K) (44), it is to be expected that render mortars with

higher EPS proportion will have the lowest thermal conductivity. Table 7 presents the results of thermal conductivity, where the proposed mixes A4, A7, A9 had a lower thermal conductivity than commercial mix AC1. In turn, as expected, mix A4 (35% EPS) was found to have the lowest conductivity values. On comparing the conductivity values of the proposed mixes with AC1, a decrease in this property was found of 79.5%, 62.3% and 71.7% for A4, A7 and A9 respectively. Mixes A4 and A9 gave lower thermal conductivity when compared to other thermal insulating materials with EPS particles (28, 29, 44, 45). The thermal conductivity in this research are similar to EPS-gypsum composites 0.18-0.24 W/m·K (30, 41), vermiculite-gypsum composites-sunflower stalk composites (27); and is lower than mortar elaborate with vermiculite-gypsum (26), 100% glass particles wastes (0.5 W/m·K) and recycled concrete aggregate (0.9-1.3 W/m·K) (46).

It was found that the selected mixes A4, A7 and A9 have a lower specific heat than commercial mix AC1, which means that in the proposed mixes a lower supply of heat energy is required to increase their temperature. The higher specific heat of the A4 mix compared to the other mixes is directly related to the higher content of EPS in the mix, since this has a higher specific heat than natural or recycled aggregates, which in turn allowed a lower thermal conductivity in A4. However, the heat transfer through the thickness of the material is slower in the proposed mixes than in AC1, due to the lower thermal diffusivity of the produced mixes, A9 being the one with the lowest thermal diffusion among the proposed mixes, which is related to the low density of the mix. The proposed mixes have a lower thermal inertia compared to mortar AC1, which indicates that their temperature can increase faster on the surface during an outbreak of fire. However, when compared with materials commonly used in interior construction, plasterboard (386 J/m² s^{1/2}K), cellular concrete (372,7 J/m² s^{1/2}K), and chipboard (226 J/m² s^{1/2}K) show close values (47, 48). Based on UNE-EN-998-1 render mortar A4 and A7 could be classified as type T2 (thermal conductivity < 0.2 W/m·K).

TABLE 7. Thermal properties of the optimized render mortars.

Mortar	Thermal conductivity (W/m·K)	Reduction vs. commercial AC1 (%)	Volumetric specific heat (MJ/m ³ ·K)	Thermal diffusivity (mm ² /s)	Specific heat (J/kg·K)	Thermal inertia (J/m ² s ^{1/2} ·K)
A4	0.1213 ± 0.0184	79.5	0.7208	0.1880 ± 0.0227	655.82 ± 0.0611	296
A7	0.2226 ± 0.0123	62.3	0.9851	0.2277 ± 0.0299	536.40 ± 0.0917	468
A9	0.1672 ± 0.0013	71.7	1.0404	0.1616 ± 0.0133	520.52 ± 0.0977	417
AC1	0.5912 ± 0.0365	--	1.2610	0.4706 ± 0.0345	522.90 ± 0.0936	863

Figure 8 correlates the results of thermal conductivity vs apparent density of the material. A directly proportional relationship can be observed between the density of the material and the thermal conductivity. As the density of the material decreases, its thermal conductivity decreases. This is directly related to a greater volume of pores that the use of recycled aggregates gives the material, which in turn causes a decrease in density and greater water absorption. The thermal conductivity in a ceramic material decreases as its density decreases (49) therefore, the percentage of water absorption increases, and the pore volume increases which means a higher content of air that acts as a heat flow barrier due to its low thermal conductivity (0.026 W/m·K).

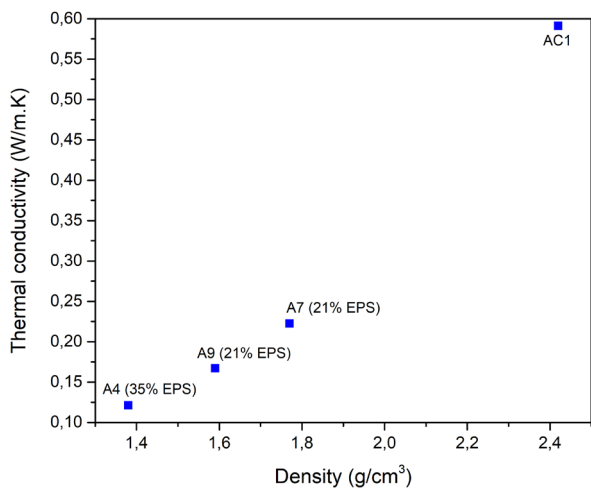
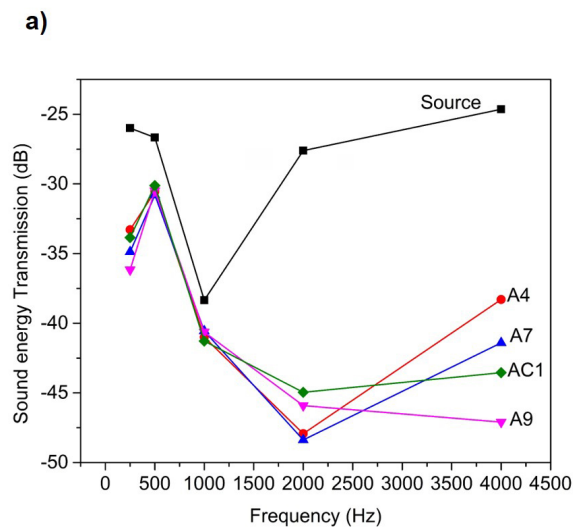


FIGURE 8. Thermal conductivity vs apparent density of the mixes.

3.7. Acoustic properties

Figure 9a shows the results of sound pressure level (SPL) measurement relative to full scale (dBFS)



for the mixes evaluated and the direct sound source, for frequencies between 250 - 4000 Hz. It must be made clear that, since the measurement is recorded relative to full scale (dBFS), the values are negative. The more the value is increased, this signifies a lower SPL. It was found in relation to the SPL of the direct sound source, the greatest reduction was achieved in general for the frequencies of 2000 Hz and 4000 Hz. A significant reduction was achieved for the frequency of 250 Hz. In contrast, for the frequencies of 500 Hz and 1000 Hz, in general, the mixes evaluated did not register a significant decrease in SPL. Figure 9b presents the results for the absorption coefficient of the developed render mortars. The A9 mix achieved the highest acoustic absorption coefficient for the frequencies of 250 Hz and 4000 Hz (0.39 and 0.91 respectively), while the A4 and A7 mixes achieved the highest acoustic absorption coefficient for the frequencies of 500 Hz (0.15 for both) and 2000 Hz (0.74 and 0.75 respectively). Among the proposed mixes, in general the acoustic absorption coefficient was low for frequencies of 500 Hz and 1000 Hz. In contrast, (29) reported acoustic absorption coefficients close to 0.7 for frequencies of 300 at 500 Hz and close to 0.5 for a frequency of 1000 Hz, for a geopolymeric cement incorporating 4% (weight) EPS with a particle size of 2.35 mm. In general, the proposed samples had a higher acoustic absorption coefficient compared to the commercial mix AC1 for frequencies of 250, 500, 2000 and 4000 Hz. This is related to the higher permeable pore volume percentage and low density of the proposed mix samples compared to AC1 (50).

In accordance with the classification of the ISO 11654-1997 standard, the proposed mixes have an *Absorbent (Class D)* behavior for frequencies of 250 Hz, *Slightly absorbent (Class E)* for 500 Hz, *Reflective* for 1000 Hz, and *Highly absorbent (Class C)* for frequencies of 2000 Hz and 4000 Hz. Only for mix A9 is

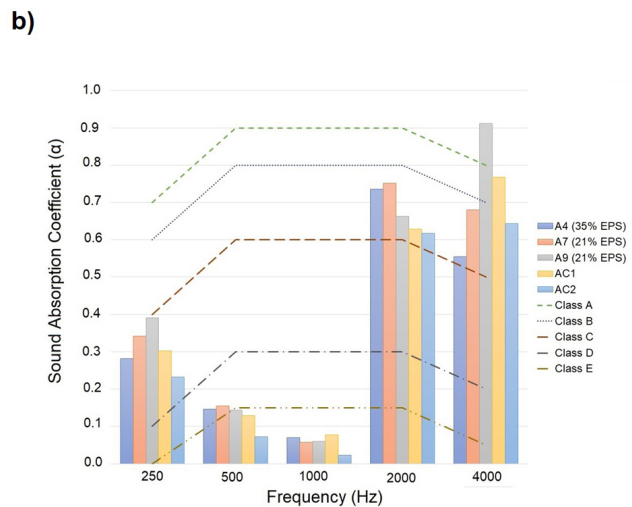


FIGURE 9. Acoustic properties, (a) Sound energy transmission for render mortar A4, A7, A9 compared to AC1, and (b) Sound absorption coefficient.

it *Extremely absorbent (Class A)* for a frequency of 4000 Hz. This can be related to the fact that, at high frequencies, the waveform lengths are smaller, so they can more easily enter the pores of the material, which is why the materials can better absorb sounds.

3.8. Application of render mortars

Application of the proposed mixes A4, A7 and A9 along with the commercial mix AC1 was carried out. In Table 8 the results of the estimated consumption of material to cover a section on a brick wall of 0.40 m x 0.50 m to two layers approximately 1 mm thick each are presented (Figure 10). It is known that the lower density contributes to the enhanced workability for the similar consistency of concrete mixtures (11). It was found that mix A4 had the lowest consumption of material and the highest demand for water. Mixes A7 and A9 had a similar consumption. The commercial mix AC1 had a higher consumption and waste of material, compared to

a lower consumption of water. The proposed mixes allow a reduction in material consumption of at least 51% compared to AC1. This is associated with the results of the apparent density test, in which it was shown that the proposed mixes have a lower density than the commercial mix. In addition, there is a directly proportional relationship between the apparent density of the material and consumption during application. The use of EPS waste allows, in addition to reducing the density of the material, lowering the consumption of material during application, which constitutes a technical and possibly economic advantage for the end user of the material, compared to the use of a traditional render mortar, corroborating what was reported by (20).

From the proposed mixes, the best workability (lower sliding resistance by the applicator trowel and better surface quality) during application was for A9. However, difficulties arose during the dispersion of the mix on the brick surface. The best workability in mix A9 can be related to the high MW content in this mix compared to A4 and A7. MW, according to the results of the particle size distribution, had a bimodal

TABLE 8. Material consumption and setting time test results for mixtures A4, A7, A9 compared to AC1.

Mortar	Solid:water ratio (parts by weight)	Consumption of material (kg/m ² /mm thickness)	Reduction in consumption compared to AC1 (%)	Initial drying time (min)	Initial setting time (min)	Final drying time (h)	Final setting time (h)
A4 (35% EPS)	1: 1.11	1.04	56%	40	1330.4	4	50.7
A7 (21% EPS)	1: 0.66	1.16	51%	40	237.6	4	27.3
A9 (21% EPS)	1: 0.75	1.17	51%	40	69.8	4	28.3
AC1	1: 0.34	2.37	---	30	37.3	2	3.3



FIGURE 10. Applied mixes, photo at day 60 (from left to right: AC1, A4, A7, A9).

distribution of particles (Figure 4b), thus providing a better distribution between the fine and coarse particles, allowing the finer ones to fill the spaces between the coarse particles, resulting in better dispersion during application to the surface. According to Weymouth's gradation theory, in order to obtain adequate workability in mortars and concretes, grains of a single size must have enough space to move within the space left by grains of the subsequent larger size. When this occurs, the particles can move freely and are better distributed in the mortar, making it extremely workable (16).

Comparing the data reported for initial drying with those reported for initial setting time (standardized method for cement), it was found that, during the actual application of the material, the initial drying time is less than the initial setting time. This is associated with the fact that the render of applied material are a few millimeters (2 mm), which allows a faster evaporation of water compared to the experimental procedure of the Vicat needle setting time test. In the case of the final drying time compared to the final setting time, the differences are more evident. During the drying time test, in the external application the proposed mixes took a maximum of 240 minutes to dry, while in the final setting time test, they took more than 24 hours, even 50 hours (mix A4). There is evidently a directly proportional relationship between the initial setting time and the EPS content in the mix, since the higher the EPS content, as in the case of mix A4 (35%), the greater the initial setting time versus mixes A7 and A9 (21%).

4. CONCLUSIONS

- Different mixes of render mortars with thermal insulation and acoustic absorption properties were produced using different waste materials such as clay brick, masonry mortar and EPS, employed as fine aggregates. The formulations A4, A7 and A9 could be considered suitable for use as interior render mortar type CS-I-W0 classification of the UNE EN-998-1 standard.
- It was identified that using BW, MW together with EPS in the mixes influences the thermal conductivity compared to the commercial mix AC1. Mix A4 and A9 (classified as type T2 according to UNE EN 998-1), which were found to have low thermal conductivity (0.12 W/m·K and 0.16 W/m·K), those achieved a 79.5% and 71.71% reduction compared to AC1, respectively. The proposed mixes A4, A7, A9 were found to be an *Absorbent* material for the frequency of 250 Hz, *Slightly absorbent* for the frequency of 500 Hz, *Reflective* for the frequency of 1000 Hz, and *Highly Absorbent* for the frequencies of 2000 Hz and 4000 Hz. Mix A9 can be considered an *Extremely absorbent* material for the frequency of 4000 Hz.
- The incorporation of EPS fillers lending the mortars a decrease in their density (1240-1590 kg/m³), further allows a lower consumption of material during application (1.04-1.17 kg/m²/mm) compared to the commercial mix AC1 (2.37 kg/m²/mm), achieving a reduction in consumption of up to 56% for utilization of A4 mortar. A full-scale development of this technological proposal could contribute to mitigating the environmental impacts derived from the high volumes of generation and final disposal of BW, MW and EPS, by allowing their reincorporation into the production cycle as raw material to produce interior render mortars, which constitutes an industrial symbiosis alternative, contributing positively to circular economy processes in the construction sector worldwide.

ACKNOWLEDGEMENT

The authors would like to extend thanks to the Universidad del Valle, and special Hernán Sánchez, Yeison Castro, and Fabian Campo for moral supporting during this research.

Funding: Universidad del Valle, Cali-Colombia.

AUTHOR CONTRIBUTIONS:

Conceptualization: C.D. Acevedo-Sánchez, M.A. Villaquirán-Caicedo, L.F. Marmolejo-Rebellón. Investigation: C.D. Acevedo-Sánchez. Methodology: C.D. Acevedo-Sánchez. Supervision: M.A. Villaquirán-Caicedo, L.F. Marmolejo-Rebellón. Writing, original draft: C.D. Acevedo-Sánchez. Writing, review & editing: M.A. Villaquirán-Caicedo, L.F. Marmolejo-Rebellón.

DECLARATION OF COMPETING INTEREST

The authors declare that they have no known competing financial interests or personal relationships that could have appeared to influence the work reported in this paper.

REFERENCES

1. Duan, P.; Song, L.; Yan, C.; Ren, D.; Li, Z. (2017) Novel thermal insulating and lightweight composites from metakaolin geopolymer and polystyrene particles. *Ceram. Int.* 43 [6], 5115–5120. <https://doi.org/10.1016/j.ceramint.2017.01.025>.
2. Domínguez, A.; Domínguez, M.I.; Ivanova, S.; Centeno, M.A.; Odriozola, J.A. (2016) Recycling of construction and demolition waste generated by building infrastructure for the production of glassy materials. *Ceram. Int.* 42 [14], 15217–15223. <https://doi.org/10.1016/j.ceramint.2016.06.157>.
3. Aghdam, K.A.; Rad, A.F.; Shakeri, H.; Sardroud, J.M. (2018) Approaching green buildings using eco-efficient construction materials: a review of the state-of-the-art. *J. Constr. Eng. Proj. Manag.* 8 [3], 1–23. <https://doi.org/10.6106/JCEPM.2018.8.3.001>.
4. Wu, H.; Zuo, J.; Zillante, G.; Wang, J.; Yuan, H. (2019) Status quo and future directions of construction and demolition

- waste research: A critical review. *J. Clean. Prod.* 240, 118163. <https://doi.org/10.1016/j.jclepro.2019.118163>.
5. Akhtar, A.; Sarmah, A.K. (2018) Construction and demolition waste generation and properties of recycled aggregate concrete: A global perspective. *J. Clean. Prod.* 186, 262–281.
 6. Wang, X.; Yu, R.; Shui, Z.; Song, Q.; Liu, Z.; Bao, M.; Liu, Z.; Wu, S. (2019) Optimized treatment of recycled construction and demolition waste in developing sustainable ultra-high performance concrete. *J. Clean. Prod.* 221, 805–816. <https://doi.org/10.1016/j.jclepro.2019.02.201>.
 7. Vincent, T.; Guy, M.; Louis-César, P.; Jean-François, B.; Richard, M. (2022) Physical process to sort construction and demolition waste (C&DW) fines components using process water. *Waste Manag.* 143, 125–134. <https://doi.org/10.1016/j.wasman.2022.02.012>.
 8. 3RMCDQ. (2017) Évaluation des alternatives de valorisation des résidus de criblage fin issus des centres de tri des débris de construction, de rénovation et de démolition. Quebec. Retrieved from www.3rmcdq.qc.ca.
 9. Reciclados Industriales. Bogotá. (2019) Retrieved from <https://recicladosindustriales.co/>.
 10. Ecotech, G. CDW Disposal System GEPECOTECH. (2022). Retrieved from https://www.gepecotech.com/solution/construction-demolition-waste-system.html?utm_source=google&utm_medium=g&utm_campaign=cdwaste&utm_content=649540851337&utm_term=demolition+waste+recycling&match=p&item=&target=kwd-3920165559&device=c&gclid=CjwKCAjwiOCgB.
 11. Şimşek, O.; Pourghadri H.; Gökçe, H.S. (2022) Performance of fly ash-blended Portland cement concrete developed by using fine or coarse recycled concrete aggregate. *Constr. Build. Mater.* 357, 129431. <https://doi.org/10.1016/j.conbuildmat.2022.129431>.
 12. Ferreira, R.L.S.; Anjos, M.A.S.; Ledesma, E.F.; Pereira, J.E.S. and Nóbrega, A.K.C. (2020) Evaluation of the physical-mechanical properties of cement-lime based masonry mortars produced with mixed recycled aggregates. *Mater. Constr.* 70 [337], e210. <https://doi.org/10.3989/mc.2020.02819>.
 13. López Ruiz, L.A.; Roca Ramón, X.; Gassó Domingo, S. (2020) The circular economy in the construction and demolition waste sector – A review and an integrative model approach. *J. Clean. Prod.* 248, 119238. <https://doi.org/10.1016/j.jclepro.2019.119238>.
 14. Kumar, G.; Shrivastava, S.; Gupta, R.C. (2020) Paver blocks manufactured from construction & demolition waste. *Mater. Today Proc.* 27, 311–317. <https://doi.org/10.1016/j.matpr.2019.11.039>.
 15. Garg, N.; Shrivastava, S. (2022) A review on utilization of recycled concrete aggregates (RCA) and ceramic fines in mortar application. *Mater. Today Proc.* 73, 64–73. <https://doi.org/10.1016/j.matpr.2022.09.226>.
 16. Miranda, L.F.R.; Selmo, S.M.S. (2006) CDW recycled aggregate renderings: Part I - Analysis of the effect of materials finer than 75 µm on mortar properties. *Constr. Build. Mater.* 20 [9], 615–624. <https://doi.org/10.1016/j.conbuildmat.2005.02.025>.
 17. Braga, M.; Brito, J.; Veiga, R. (2012) Incorporation of fine concrete aggregates in mortars. *Constr. Build. Mater.* 36, 960–968. <https://doi.org/10.1016/j.conbuildmat.2012.06.031>.
 18. Silva, R.V.; Brito, J.; Dhir, R.K. (2016) Performance of cementitious renderings and masonry mortars containing recycled aggregates from construction and demolition wastes. *Constr. Build. Mater.* 105, 400–415. <https://doi.org/10.1016/j.conbuildmat.2015.12.171>.
 19. Jesus, S.; Maia, C.; Brazão Farinha, C.; Brito, J.; Veiga, R. (2019) Rendering mortars with incorporation of very fine aggregates from construction and demolition waste. *Constr. Build. Mater.* 229, 116844. <https://doi.org/10.1016/j.conbuildmat.2019.116844>.
 20. Ferreira, R.L.S.; Anjos, M.A.S.; Nóbrega, A.K.C.; Pereira, J.E.S.; Ledesma, E.F. (2019) The role of powder content of the recycled aggregates of CDW in the behaviour of rendering mortars. *Constr. Build. Mater.* 208, 601–612. <https://doi.org/10.1016/j.conbuildmat.2019.03.058>.
 21. Deer, R. (2021) Styrofoam an environmental problem? RoadRunner. Retrieved from <https://www.roadrunnerwm.com/blog/styrofoam-problems-and-how-to-help#:~:text=Most recycling facilities are unable is time-consuming and expensive>.
 22. EPA. (2022) Containers and packaging United States Environmental Protection Agency. Retrieved from <https://www.epa.gov/facts-and-figures-about-materials-waste-and-recycling/containers-and-packaging-product-specific>.
 23. Cácerres, M.A.; Sánchez, M.; Soto, M.; Maspoch, L.; Sánchez Hernández, M.; Sánchez Rojo, A. (2015) Desarrollo de un proceso de reciclaje para la fracción mixta de residuos de plástico, provenientes de plantas de separación selectiva. in II Congreso UPC Sostenible. Retrieved from <https://upcommons.upc.edu/handle/2099/8207?show=full>.
 24. World centric for a better world (2019) Impacts and risks of polystyrene. <https://www.worldcentric.com/journal/impacts-and-risks-of-styrofoam>.
 25. Morales, M.P.; Muñoz, P.; Juárez, M.C.; Mendivil, M.A.; Olasolo, P. (2016). Influence of the type of lightweight clay brick on the equivalent thermal transmittance of different types of façades on buildings. *Mater. Construcc.* 66 [323], e096. <https://doi.org/10.3989/mc.2016.08115>.
 26. Gencel, O.; Coz Diaz, J.J.; Stcu, M.; Koksall, F.; Alvarez, F.P.; Martinez-Barrera, G.; Brostow, W. (2014) Properties of gypsum composites containing vermiculite and polypropylene fibers: Numerical and experimental results. *Energy Build.* 70, 135–144. <https://doi.org/10.1016/j.enbuild.2013.11.047>.
 27. Binici, H.; Aksogan, O.; Dincer, A.; Luga, E.; Eken, M.; Isikaltun, O. (2020) The possibility of vermiculite, sunflower stalk and wheat stalk using for thermal insulation material production. *Therm. Sci. Eng. Prog.* 18 [21], 100567. <https://doi.org/10.1016/j.tsep.2020.100567>.
 28. Fernández, D.; Yedra, E.; Morón, C.; Zaragoza, A.; Kosior-Kazberuk, M. (2022) Circular building process: reuse of insulators from construction and demolition waste to produce lime mortars. *Buildings.* 12 [2], 220. <https://doi.org/10.3390/buildings12020220>.
 29. Villalquirán-Cacedo, M.A.; Perea, V.N.; Ruiz, J.E.; Mejía de Gutiérrez, R. (2022) Mechanical, physical and thermoacoustic properties of lightweight composite geopolymers. Propiedades mecánicas, físicas y termoacústicas de geopolímeros compuestos aligerados. *Ingen. Compet.* 24 [1], 1–21.
 30. Oliveira, K.A.; Oliveira, C.A.B.; Molina, J.C. (2021) Lightweight recycled gypsum with residues of expanded polystyrene and cellulose fiber to improve thermal properties of gypsum. *Mater. Construcc.* 71 [341], e242. <https://doi.org/10.3989/mc.2021.07520>.
 31. Fraile-García, E.; Ferreira-Cabello, J.; Defez, B.; Peris-Fajanes, G. (2016) Acoustic behavior of hollow blocks and bricks made of concrete doped with waste-tire rubber. *Mater.* 9 [12], 962. <https://doi.org/10.3390/ma9120962>.
 32. Holmes, N.; Browne, A.; Montague, C. (2014) Acoustic properties of concrete panels with crumb rubber as a fine aggregate replacement. *Constr. Build. Mater.* 73, 195–204. <https://doi.org/10.1016/j.conbuildmat.2014.09.107>.
 33. Orrego González, A.; Ealo Cuello, J.L.; Pazos Ospina, J.F. (2018) Low-cost and easily implemented anechoic acoustic chambers. *Sci. Tech.* 23 [4], 471–478.
 34. Ferreira, R.L.S.; Anjos, M.A.S.; Maia, C.; Pinto, L.; Azevedo, A.R.; Brito, J. (2021) Long-term analysis of the physical properties of the mixed recycled aggregate and their effect on the properties of mortars. *Constr. Build. Mater.* 274, 121796. <https://doi.org/10.1016/j.conbuildmat.2020.121796>.
 35. Bonifazi, G.; Palmieri, R.; Serranti, S. (2018) Evaluation of attached mortar on recycled concrete aggregates by hyperspectral imaging. *Constr. Build. Mater.* 169, 835–842. <https://doi.org/10.1016/j.conbuildmat.2018.03.048>.
 36. Kim, J. (2022) Influence of quality of recycled aggregates on the mechanical properties of recycled aggregate concretes: An overview. *Constr. Build. Mater.* 328, 127071. <https://doi.org/10.1016/j.conbuildmat.2022.127071>.
 37. Sayadi, A.A.; Tapia, J.V.; Neitzert, T.R.; Clifton, G.C. (2016) Effects of expanded polystyrene (EPS) particles on fire resistance, thermal conductivity and compressive strength of foamed concrete. *Constr. Build. Mater.* 112, 716–724. <https://doi.org/10.1016/j.conbuildmat.2016.02.218>.

38. Zawrah, M.F.; Gado, R.A.; Feltin, N.; Ducourtieux, S.; Devoille, L. (2016) Recycling and utilization assessment of waste fired clay bricks (Grog) with granulated blast-furnace slag for geopolymer production. *Process Saf. Environ. Prot.* 103, 237–251. <https://doi.org/10.1016/j.psep.2016.08.001>.
39. Fernández-Ledesma, E.; Jiménez, J.R.; Ayuso, J.; Corinaldesi, V.; Iglesias-Godino, F.J. (2016) A proposal for the maximum use of recycled concrete sand in masonry mortar design. *Mater. Construcc.* 66 [321], e075. <https://doi.org/10.3989/mc.2016.08414>.
40. Fernández-Ledesma, E.; Jiménez, J.R.; Ayuso, J.; Fernández, J.M.; Brito, J. (2015) Maximum feasible use of recycled sand from construction and demolition waste for eco-mortar production - Part-I: Ceramic masonry waste. *J. Clean. Prod.* 87 [1], 692–706. <https://doi.org/10.1016/j.jclepro.2014.10.084>.
41. Bumanis, G.; Pavils, P.; Sahmenko, G.; Mironovs, D.; Rucevskis, S.; Korjakins, A.; Bajare, D. (2023) Thermal and sound insulation properties of recycled expanded polystyrene granule and gypsum composites. *Recycling*. 8 [1], 19. <https://doi.org/10.3390/recycling8010019>.
42. Saiz Martínez, P.; González Cortina, M.; Fernández Martínez, F.; Rodríguez Sánchez, A. (2016). Comparative study of three types of fine recycled aggregates from construction and demolition waste (CDW), and their use in masonry mortar fabrication. *J. Clean. Prod.* 118, 162–169. <https://doi.org/10.1016/j.jclepro.2016.01.059>.
43. Patra, I.; Al-Awsi, G.R.L.; Hasan, Y.M.; Almotlaq, S.S.K. (2022) Mechanical properties of concrete containing recycled aggregate from construction waste. *Sustain. Energy Technol. Assessments*. 53, 102722. <https://doi.org/10.1016/j.seta.2022.102722>.
44. Fernández, D.; Álvarez, M.; Saiz, P.; Zaragoza, A. (2022) Experimental study with plaster mortars made with recycled aggregate and thermal insulation residues for application in building. *Sustain.* 14 [4], 2386. <https://doi.org/10.3390/su14042386>.
45. Villaquirán-Cañedo, M.A.; Mejía de Gutierrez, R.; Sulekar, S.; Davis, C.; Nino, J. (2015) Thermal properties of novel binary geopolymers based on metakaolin and alternative silica sources *Appl. Clay Sci.* 118, 276–282. <https://doi.org/10.1016/j.clay.2015.10.005>.
46. Chindapasirt, P. (2022) Thermal insulating and fire resistance performances of geopolymer mortar containing auto glass waste as fine aggregate. *J. Build. Eng.* 60, 105178. <https://doi.org/10.1016/j.jobe.2022.105178>.
47. Balaji, N.C.; Mani, M.; Reddy, B.V. (2013) Thermal performance of the building walls. In 1st IBPSA Italy Conference Free University of Bozen-Bolzano. 346, 1–8. Retrieved from <http://www.ibpsa.org/bsa-2013-bozen-bolzano-italy-conference-proceedings/>.
48. Serna Jara, L.M. (2016) Research study against high intensity fireworks for pipeline conductions in the petrochemical industry. *Rev. Dr. UMH*, 2 [1], 1–10. Retrieved from <https://revistas.innovacionumh.es/index.php/doctorado/article/view/615/966>.
49. Gregorová, E.; Pabst, W.; Sofer, Z.; Jankovský, O.; Matějčíček, J. (2012) Porous alumina and zirconia ceramics with tailored thermal conductivity. *J. Phys. Conf. Ser.* 395, 012022. <https://doi.org/10.1088/1742-6596/395/1/012022>.
50. Moretti, E.; Belloni, E.; Agosti, F. (2016) Innovative mineral fiber insulation panels for buildings: Thermal and acoustic characterization. *Appl. Energy*, 169, 421–432. <https://doi.org/10.1016/j.apenergy.2016.02.048>.